JOURNAL OF GUIDANCE, CONTROL, AND DYNAMICS
Vol. 25, No. 3, May–June 2002

Predictor/Flight-Path Display for Manual Longitudinal Control Improvement

G. Sachs* and K. Dobler†
Technical University of Munich, 85747 Garching, Germany

A predictor can substantially enhance the guidance and control capabilities possible with a perspective flight-path display. A new predictor concept based on manual control theory and related pilot-centered requirements is introduced for the longitudinal motion to achieve best performance for manual control of the predictor-aircraft system. Key predictor factors are identified and optimized. The new predictor concept requires minimum compensatory effort by the pilot and features insensitivity to turbulence. It also provides a high degree of face validity for displaying guidance information in a descriptive and three-dimensional format. The conceptual and theoretic control findings are verified with pilot-in-the-loop simulation experiments.

Nomenclature

e_{PR}	=	predictor position error
g	=	acceleration caused by gravity
h	=	altitude
K	=	gain
M	=	pitching moment
q	=	pitch rate
s	=	Laplace operator
T	=	time constant
T_{PR}	=	prediction time
t	=	time
V	=	speed
$Y(s)$	=	transfer function
Z	=	vertical force
γ	=	flight-path angle
Δ	=	perturbation, e.g., Δh
δ_e	=	pitch control deflection
ζ	=	damping ratio
τ_e	=	effective time delay
ω	=	frequency

Introduction

A PERSPECTIVE flight-path display with a predictor is a promising new concept for an advanced cockpit instrumentation. It has potential for a substantial enhancement in the guidance and control of aircraft. This is because a perspective flight-path display with a predictor provides the pilot with visual information of the command flight path and the future position of the aircraft in a three-dimensional format. By contrast, current instrumentation merely yields a planar picture basically related to the current state of the aircraft. A mental effort is required by the pilot to reconstruct the spatial and temporal situation.

Recent developments in the field of perspective flight-path displays have led to significant progress, which is documented in theoretical and experimental investigations (Refs. 1–15). The experimental investigations include both simulation experiments and flight tests. In a dedicated flight-test series the first landing of an aircraft with a pictorial display presenting three-dimensional guidance information (Computer Generated Synthetic Vision) as the only visual information for the pilot was achieved.[12,13] The results attained with perspective flight-path displays show that significant improvements in guidance and control are possible.

In the research thus far emphasis was placed on the lateral motion of aircraft and corresponding guidance and control issues of predictive displays, which have been treated in great detail.[1,3–7,10,14,15] The advantage of a predictor for lateral control was demonstrated by theoretical investigations and experimental evaluations with pilot-in-the-loop simulations and flight tests. Research subjects for lateral predictor control include various predictor laws, simple or complex predictor information, pilot-vehicle stability analysis, and improved reference guidance information.[3–7] With regard to predictive information, Ref. 16 is of interest because it presents a predictor the dynamics of which are designed to yield desirable transfer characteristics for longitudinal and lateral control. Furthermore, manual control theory is used to improve control performance and to achieve lateral predictor-aircraft system characteristics requiring minimum pilot compensation.[14,15]

In contrast to the detailed treatment of lateral control, less attention has been directed to the specific problems of longitudinal control and the related potential of perspective flight-path displays with predictor. A recommendation is expressed in Ref. 4 for developing improvements, enabling a more accurate vertical path-angle control. Furthermore, turbulence sensitivity appears to be an issue for longitudinal predictors (as opposed to lateral predictors).

The purpose of this paper is to show that perspective flight-path/predictor displays offer a significant improvement for manual longitudinal control. For achieving this goal, manual control theory is used, and appropriate pilot-centered requirements are specified. It will be shown that longitudinal control poses unique predictor problems that substantially differ from those of lateral control. These problems concern the dynamic characteristics of the controlled predictor-aircraft element from the standpoint of manual control. Another problem is the possible sensitivity of the longitudinal predictor-aircraft system to turbulence. For the addressed problems solutions will be presented.

Pilot-Centered Requirements for Compensatory Predictor Control

A perspective flight-path display with a predictor provides the pilot with information about the future position of the aircraft and the command trajectory in a three-dimensional format (Fig. 1). The predictor shows the future position at the prediction time ahead, and the command flight path is presented in the form of a tunnel. The predictor provides a precise indication of the position error if referenced to the corresponding cross section of the tunnel. This cross section, which shows the command position at the prediction time ahead, is indicated by a special marking.

When the pilot acts in response to the error of the predictor position, he operates in a compensatory control mode. This is a main

Received 8 October 1999; revision received 18 August 2000; accepted for publication 19 August 2000.

*Director, Institute of Flight Mechanics and Flight Control, Boltzmannstr. 15. Fellow AIAA.

†Research Assistant, Institute of Flight Mechanics and Flight Control, Boltzmannstr. 15.

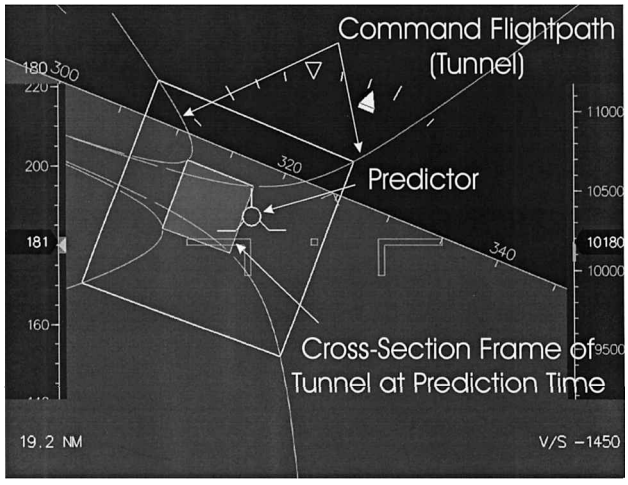

Fig. 1 Predictive flight-path display with three-dimensional flight-path presentation.

control possibility offered by the predictor of the perspective flight-path display. Accordingly, compensatory control of the predictor-aircraft system by the pilot is the subject of this paper. Though predictor control originally concerns an error state in the future at the prediction time ahead, it will be shown that compensatory control related to the predictor is also very efficient for minimizing the error of the current state.

Compensatory control of the predictor-aircraft system by the pilot is an issue of manual control, where the pilot operates on visually sensed inputs and exerts manual control outputs. Manual control theory shows that there are pilot-centered requirements for achieving best results in terms of performance and workload by the pilot. Based on these requirements, a proper design of the predictor can be achieved.

A primary goal is a predictor design that requires minimum compensatory effort by the pilot and provides maximum system performance. From manual control theory it is known which dynamic properties the controlled element should have for achieving this goal.[17,18] This can be summarized as a design requirement for constructing the controlled element to yield the following properties: 1) no low-frequency lead equalization required for the pilot and 2) pilot loop closure possible over a wide range of gains. These results can be achieved when the controlled element, which is the predictor-aircraft system $Y_{PR}(s)Y_C(s)$, approximates either a pure gain or a pure integration over an adequately broad region centered around pilot-predictor-aircraft crossover, that is,

Pure gain:

$$Y_{PR}(s)Y_C(s) = K \tag{1}$$

Pure integration:

$$Y_{PR}(s)Y_C(s) = K/s \tag{2}$$

The integration characteristic K/s is nearly as good as a pure gain K with regard to pilot response and performance. It has distinct advantages over the pure gain as a basis for the design of the predictor. This will be shown in subsequent sections.

There are further dynamic requirements that are of concern for the pilot-predictor-aircraft system: 1) system stability, 2) response quality, 3) turbulence sensitivity, and 4) face validity.

Basic Predictor (Circular Flight-Path Continuation)

A predictor indicates the future position of the aircraft at the prediction time ahead (Fig. 1). The predicted position is based on an estimation of the future flight path on which the aircraft would proceed (as opposed to the command flight path). There are various models for flight-path estimation in use, relying on geometric/kinematic relations of different order. A promising model used in recent research is referenced to a circular continuation of the current flight path.[1,3–8,10,14,15] Geometric and kinematic relationships of a circular

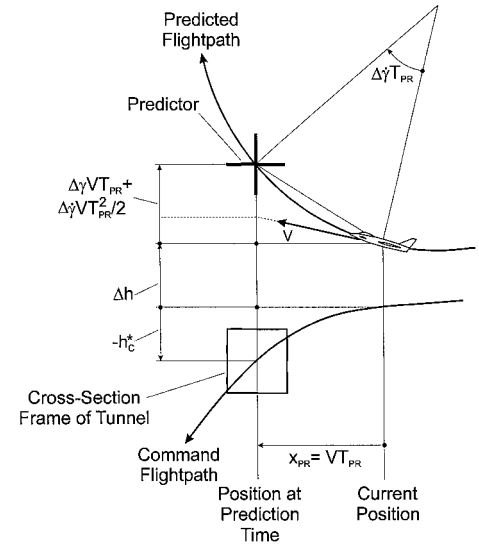

Fig. 2 Displacement of basic predictor (circular flight-path continuation).

flight-path continuation are shown in Fig. 2. Accordingly, the displacement of the predicted position from the command flight path at the prediction time T_{PR} ahead can be described with the following relation:

$$\Delta h_{PR} = \Delta h - h_C^* + VT_{PR}\Delta\gamma + V\left(T_{PR}^2/2\right)\Delta\dot{\gamma} \tag{3}$$

The displacement of the predicted position can be determined with quantities of the current aircraft motion (Fig. 3). Accordingly, the following relation holds for the displacement Δh_{PR} referenced to flight-path angle rate after Laplace transformation:

$$\Delta h_{PR}(s) = V\left(T_{PR}^2/2 + T_{PR}/s + 1/s^2\right)\Delta\dot{\gamma}(s) \tag{4}$$

The displacement Δh_{PR} is indicated by the predictor symbol in the perspective flight-path display as an error e_{PR} (Fig. 3):

$$e_{PR}(s) = K_{PR}\Delta h_{PR}(s) \tag{5}$$

Combining Eqs. (4) and (5) yields the transfer function between the flight-path angle rate and the error presented by the predictor symbol:

$$(Y_{PR})_{circular} = \frac{e_{PR}(s)}{\Delta\dot{\gamma}(s)} = K_{PR}V\frac{\left(T_{PR}^2/2\right)s^2 + T_{PR}s + 1}{s^2} \tag{6}$$

This transfer function describes the dynamic characteristics of the predictor with a circular flight-path continuation. There are two factors T_{PR} and K_{PR} that can be selected for best equalization for the controlled aircraft-predictor element.

The effect of the prediction time T_{PR} manifests in the numerator of the predictor transfer function Eq. (6) and related zeros. Because the zeros are generally complex, the numerator can be rewritten as

$$s^2 + 2\zeta_{PR}\omega_{PR}s + \omega_{PR}^2 = s^2 + (2/T_{PR})s + 2/T_{PR}^2 \tag{7}$$

where the following solution holds:

$$\omega_{PR} = \sqrt{2}/T_{PR}, \qquad \zeta_{PR} = 1/\sqrt{2} \tag{8}$$

With regard to aircraft dynamics, the short-term response behavior is of concern because it is most significant for the frequency region in mind. It is characterized by the short period mode and its frequency and damping ω_{SP} and ζ_{SP}. The following relation holds for the frequency region of concern (i.e., for pilot system crossover):

$$Y_C = \frac{\Delta\dot{\gamma}(s)}{\delta_e(s)} = -\frac{Z_\alpha M_{\delta_e}/V}{s^2 + 2\zeta_{SP}\omega_{SP}s + \omega_{SP}^2} \tag{9}$$

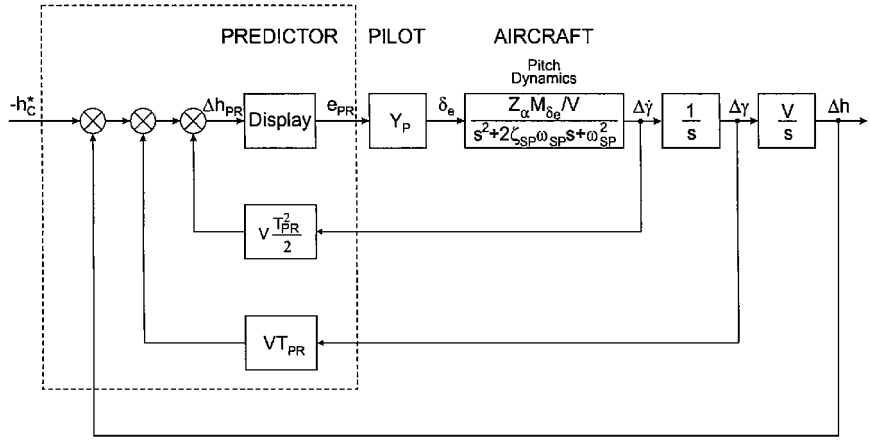

Fig. 3 Block diagram for basic predictor.

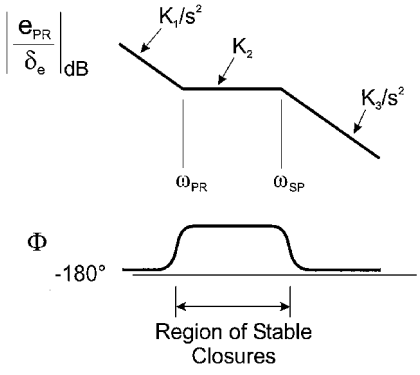

Fig. 4 Asymptotic Bode plot for predictor-aircraft system (basic predictor with circular flight-path continuation).

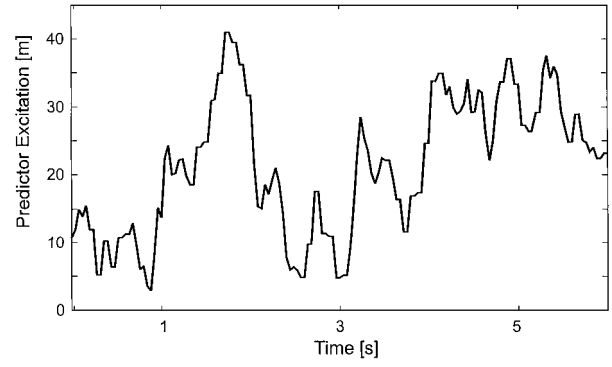

Fig. 5 Excitation of predictor position caused by turbulence (basic predictor with circular flight-path continuation).

With Eqs. (6) and (9) the open-loop transfer function of the controlled element reads (effective predictor to longitudinal control response, without pilot)

$$\left.\frac{e_{\mathrm{PR}}(s)}{\delta_e(s)}\right|_{\text{circular}} = -K_{\mathrm{PR}} Z_\alpha M_{\delta_e} \frac{T_{\mathrm{PR}}^2}{2} \frac{s^2 + 2\zeta_{\mathrm{PR}}\omega_{\mathrm{PR}} s + \omega_{\mathrm{PR}}^2}{s^2\left(s^2 + 2\zeta_{\mathrm{SP}}\omega_{\mathrm{SP}} s + \omega_{\mathrm{SP}}^2\right)} \tag{10}$$

This transfer function describes the dynamic behavior of the predictor-aircraft system, where a predictor with circular flight-path continuation is used. Its characteristics are illustrated in Fig. 4, which shows a generic Bode plot of the open-loop predictor-aircraft system. The frequency region of primary concern is the region between $\omega_{\mathrm{PR}} = \sqrt{(2)}/T_{\mathrm{PR}}$ and ω_{SP} because it can be regarded as the region where pilot system crossover occurs. Figure 4 shows that there is K characteristic in this frequency region. Thus, it can be regarded as a predictor candidate from the standpoint of controlled element transfer characteristics.

However, there are other properties of the basic predictor with circular flight-path continuation, which appear to be inadequate.

One issue is closed-loop stability. There can be a significant reduction in damping and frequency of attitude mode characteristics. An advantage in this respect can be achieved with another predictor concept considered in the following section.

A further issue is turbulence sensitivity. The basic predictor with circular flight-path continuation shows a rather great sensitivity to turbulence. This is illustrated in Fig. 5, which presents the response of the basic predictor to turbulence without a controlling action by the pilot (Dryden model with rms intensity of 4.7 ft/s for vertical and 4.85 ft/s for longitudinal gusts, according to Refs. 19 and 20, aircraft dynamics described in the following section). The results of Fig. 5 suggest that the degree of predictor motion that is excited by turbulence is rather high. The reason why the turbulence effect is so strong is because of the high gain $VT_{\mathrm{PR}}^2/2$ in the $\dot{\gamma}$ pathway (Fig. 3).

Experience and results from simulation experiments support the preceding conclusion according to which such a high degree of predictor motion excitation is very disturbing. Therefore, avoidance of the detrimental turbulence effects is a further objective.

Extended Predictor Concept

In this section a new predictor concept is introduced, which is capable of achieving the design goals just described. Emphasis is placed on two requirements: 1) to provide a transfer characteristic for minimum pilot compensation K or K/s, over an adequately broad region centered around pilot-predictor-aircraft crossover; and 2) to avoid detrimental turbulence effects.

Transfer Characteristic for Minimum Pilot Compensation

The preceding objectives can be achieved when the $\dot{\gamma}$ feedback is replaced by a q feedback, as shown in Fig. 6, and by selecting an appropriate gain for this pathway. With reference to the pathways in the block diagram of Fig. 6, the predictor position error can be expressed as

$$e_{\mathrm{PR}}(s) = K_{\mathrm{PR}}\left[\frac{K_q}{1 + T_W s}\Delta q(s) + \frac{VT_{\mathrm{PR}}s + V}{s^2}\Delta\dot{\gamma}(s)\right] \tag{11}$$

Applying the relation between $\Delta q(s)$ and $\Delta\dot{\gamma}(s)$ for pitch control inputs

$$\Delta q(s)/\Delta\dot{\gamma}(s) = 1 - (V/Z_\alpha)s = 1 + T_{\theta_2} s \tag{12}$$

the following form for the predictor transfer function results from Eq. (11):

$$Y_{\mathrm{PR}} = \frac{e_{\mathrm{PR}}(s)}{\Delta\dot{\gamma}(s)} = K_{\mathrm{PR}}\frac{\left[\left(1 + T_{\theta_2}s\right)/\left(1 + T_W s\right)\right]K_q s^2 + VT_{\mathrm{PR}}s + V}{s^2} \tag{13}$$

For T_W, the following relation is selected:

$$T_W = T_{\theta_2} \tag{14}$$

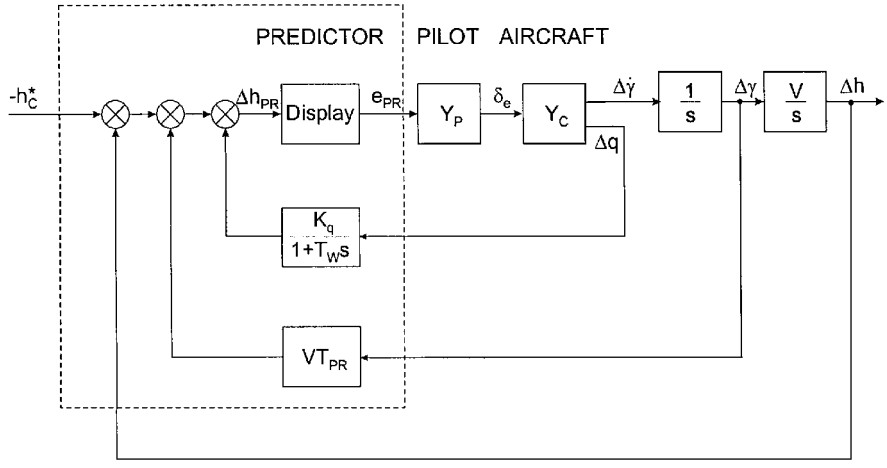

Fig. 6 Extended predictor concept.

Using this relation, Eq. (14) can be rewritten as

$$Y_{\mathrm{PR}} = \frac{e_{\mathrm{PR}}(s)}{\Delta\dot{\gamma}(s)} = K_{\mathrm{PR}} V \frac{(K_q/V)s^2 + T_{\mathrm{PR}}s + 1}{s^2} \tag{15}$$

Equation (15) shows that proper selection of T_{PR} and K_q can yield the desired K/s frequency characteristics:

1) T_{PR}, which describes the prediction time span, can be used for determining the lower end of the K/s frequency region.

2) K_q can be used for determining the upper end of K/s frequency region, such that a numerator zero is placed close to the short period frequency ω_{SP}.

These goals can be achieved if the numerator of the predictor transfer function, Eq. (15), has real zeros (instead of complex zeros as with the basic predictor). Thus, the numerator can be rewritten as

$$s^2 + T_{\mathrm{PR}}(V/K_q)s + V/K_q = (s + 1/T_1)(s + 1/T_2) \tag{16}$$

The zeros, which are ad separated in frequency for achieving the purpose in mind, that is,

$$T_2 \ll T_1$$

can be approximated by

$$T_1 \approx T_{\mathrm{PR}} \tag{17a}$$

$$T_2 \approx K_q/V T_{\mathrm{PR}} \tag{17b}$$

With Eqs. (15) and (16) the open-loop transfer function of the controlled predictor-aircraft element can be expressed as

$$\frac{e_{\mathrm{PR}}(s)}{\delta_e(s)} = -\frac{K_{\mathrm{PR}} Z_\alpha M_{\delta_e} K_q}{V} \frac{(s + 1/T_1)(s + 1/T_2)}{s^2\left(s^2 + 2\zeta_{\mathrm{SP}}\omega_{\mathrm{SP}}s + \omega_{\mathrm{SP}}^2\right)} \tag{18}$$

Resulting predictor-aircraft transfer characteristics are illustrated in Fig. 7, which shows that there is a K/s characteristic in the frequency region between $1/T_1$ and $1/T_2$. By proper selection of T_{PR} and K_q according to Eqs. (17a) and (17b), it is possible to place $1/T_2$ close to ω_{SP}. Thus, a K/s characteristic can be generated that practically extends from $1/T_1$ to ω_{SP}. This is the frequency region where pilot system crossover is possible. A K/s frequency region of sufficient length can be achieved by proper selection of T_1 in relation to ω_{SP}, thus determining T_{PR} (because $T_{\mathrm{PR}} \approx T_1$).

Placing $1/T_2$ close to ω_{SP} yields the following relation for the gain in the q pathway:

$$K_q \approx V T_{\mathrm{PR}}/\omega_{\mathrm{SP}} \tag{19}$$

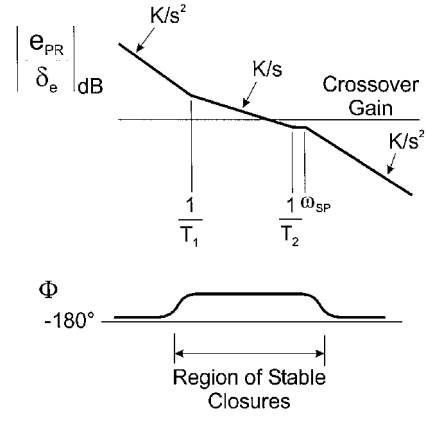

Fig. 7 Asymptotic Bode plot for predictor-aircraft system for extended predictor.

Avoidance of Detrimental Turbulence Effects

Turbulence effects are substantially reduced when compared with the basic predictor. This is because the gain K_q in the q pathway, which can be considered the most susceptible one out of the pathways used for the predictor law (Fig. 6), is significantly decreased. As a measure for the reduction of the turbulence effects, the ratio of the gains in the q and $\dot{\gamma}$ pathways of the new predictor and the basic predictor concepts (Figs. 3 and 6) may be used:

$$K_q/K_{\dot{\gamma}} = 2/\omega_{SP} T_{PR} \tag{20}$$

where K_q is given by Eq. (19). For typical values such as $T_{PR} = 5$ s and $\omega_{SP} \geq 2$ rad/s, this ratio is

$$K_q/K_{\dot{\gamma}} \leq 0.2$$

There is a further effect contributing to a reduction of the detrimental turbulence effects. It concerns the element $1/(1 + T_W s)$ in the q pathway (Fig. 6). With $T_W = T_{\theta_2}$ according to Eq. (15), the denominator term is given by $1 + T_{\theta_2}s$. This term becomes effective in the frequency range $\omega \geq 1/T_{\theta_2}$.

The effectiveness of extended predictor concept for avoiding detrimental turbulence effects is illustrated in Fig. 8. Comparison with Fig. 5, where the same turbulence characteristics are considered for the basic predictor, reveals that the new predictor approach yields a superior solution, which shows practically no turbulence excitation. This result is confirmed by results from simulation experiments where the pilots noted no objectionable turbulence effects with the extended predictor concept (as opposed to the basic predictor with circular flight-path continuation).

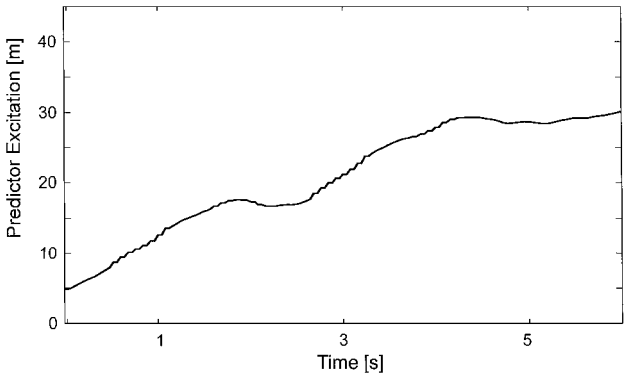

Fig. 8 Excitation of predictor position caused by trubulence for extended predictor concept.

Remarks for the Extended Predictor Concept

With regard to the new predictor concept introduced in this section, three further aspects can be considered:

1) Noncircular fligh-path continuation: From a geometry/kinematics standpoint the predictor with q feedback shows a noncircular flight-path continuation. This is because flight-path angle rate $\dot{\gamma}$ is replaced by pitch-angle rate q. Furthermore, the q feedback gain $K_q \approx VT_{PR}/\omega_{SP}$ is smaller than the $\dot{\gamma}$ feedback gain of the basic predictor $K_{\dot{\gamma}} \approx VT_{PR}^2/2$. As a consequence, the noncircular flight-path continuation differs from the circular one, showing a decreased contribution of flight-path curvature (or centripetal acceleration, respectively).

2) Face validity: Face validity concerns the correspondence between status information presented by the predictor in the perspective flight-path display and the actual situation. If there is a clear correspondence, the status information has a high degree of face validity. In this respect the predictor function is to indicate the future position of the aircraft at the prediction time ahead. The face-validity issue is considered important because the predictor is an element of a perspective flight-path display, which presents guidance information to the pilot in a descriptive and three-dimensional format.

Indication of the future position can be provided with different predictor models as long as the models provide a realistic estimation of the continuation of the flight path. The predictor with q feedback represents a predictor model that has geometric/kinematic relationships which differ from the basic predictor model with circular flight-path continuation, showing a reduced contribution of flight-path curvature. This contribution is determined on the assumption that flight-path curvature is constant throughout the entire prediction time span T_{PR}. Because there are prediction times in the order of $T_{PR} = 5$ s, a constant curvature (or constant centripetal acceleration, respectively) may not be the case. This particularly holds for short correcting control actions of the pilot for error reduction. As a consequence, there is an overestimation of the contribution of flight-path curvature if its gain is too high. A reduction in the weighting of flight-path curvature contribution can contribute to realistically estimating the position of the predictor. Thus, the predictor with q feedback can be considered a predictor model yielding correspondence between displayed status information and actual situation.

The suitability of the predictor with q feedback as a realistic predictor model with a high degree of face validity is supported by the results and the experience gained in the simulation experiments. There are no objectionable comments of the pilots from the simulation test runs.

3) Use of pitch rate q: Sensors for measuring pitch rate are simple and robust. This can be considered an advantage in terms of sensor system reliability and avoidance of complexity.

Stability and Response Quality

With the root-locus technique results of general nature can be obtained for closed-loop stability of the pilot-predictor-aircraft system. Results are presented in Fig. 9.

The open-loop pole/zero configuration of the predictor-aircraft system, which is significant for loop closure, has two zeros and

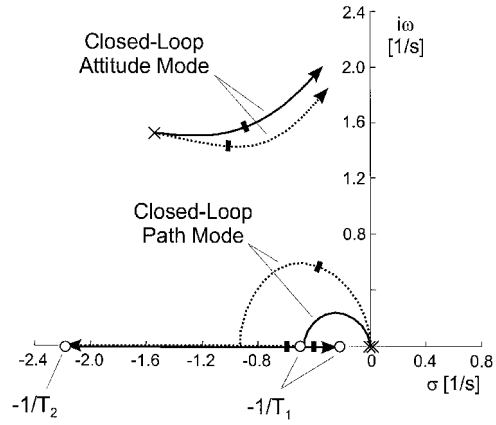

Fig. 9 Root locus of closed-loop system (extended predictor concept): $1/T_2 \approx \omega_{SP}$; pliot model Eq. (21) with $\tau_e = 0.25$ s; ▮, pilot gain from simulation experiments; ——, $T_{PR} = 5.0$ s; - - - -, $T_{PR} = 2.5$ s.

poles of the predictor [Eqs. (13–14)] and two poles of the aircraft [Eq. (8)].

For the pilot the following model is used, which is valid for systems described by a K/s characteristic in the frequency region centered around pilot system crossover frequency[17,18]:

$$Y_P(s) = K_P e^{-\tau_e s} \tag{21}$$

Figure 9 shows that there are two root-locus branches, one of which emerges from the short period poles (closed-loop attitude mode) and the other from the origin (closed-loop path mode). From the characteristics of the root-locus, it follows that the path mode is basically stable. Its damping and frequency profit from loop closure. The attitude mode, on the other hand, shows a destabilization. For the pilot gain at crossover, the closed-loop system is stable.

The described results about system stability are supported by the following approximations for the closed-loop roots, which hold for the pilot gain at crossover:

Path mode:

$$\omega'_P \approx \sqrt{\frac{\omega_C/T_{PR}}{1+\omega_C/\omega_{SP}}}, \qquad \zeta'_P\omega'_P \approx \frac{\omega_C/2}{1+\omega_C/\omega_{SP}} \tag{22}$$

Attitude mode:

$$\omega'_{SP} \approx \omega_{SP}\left[\sqrt{1+\frac{\omega_C}{\omega_{SP}}} - \frac{2\zeta_{SP}\omega_C}{1+\omega_C/\omega_{SP}}\right]$$

$$\zeta'_{SP}\omega'_{SP} \approx \zeta_{SP}\omega_{SP} - \zeta'_P\omega'_P \tag{23}$$

Figure 9 also provides an insight into response quality characteristics. The low-frequency mode represents a path mode, the properties of which are significant for flight-path control. The high-frequency mode describes the attitude behavior. For pilot loop-closure gain both modes show rapid and adequately damped response characteristics and are well separated in frequency. Furthermore, it follows from the root-locus characteristics (open-loop pole/zero configuration) that pilot loop closure does not drive the system modes into near proximity.

Experimental Verification

Experimental verification of the preceding issues was achieved with simulation experiments. For the simulation-test runs a fixed base simulator was used. It features a perspective flight-path display with predictor as shown in Fig. 1. A nonlinear six-degree-of-freedom aircraft model representative of small, twin jet-engine aircraft was used to simulate aircraft dynamics characteristics. The tasks of the pilots was to follow precisely a flight path consisting of alternating descending and ascending segments (Fig. 10). The sequence of the alternating flight-path segments was changed to avoid familiarization of the pilots with a fixed trajectory. Five pilots with a different professional background (four airline pilots and a flight instructor for motor gliders) took part in the simulation-test program.

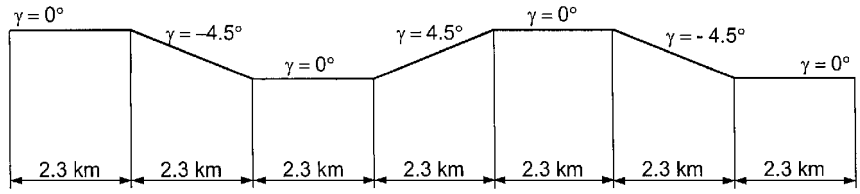

Fig. 10 Altitude profile of flight path in simulation experiments.

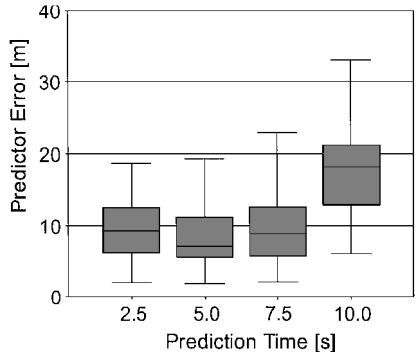

Fig. 11 Deviation of predictor position (extended predictor concept).

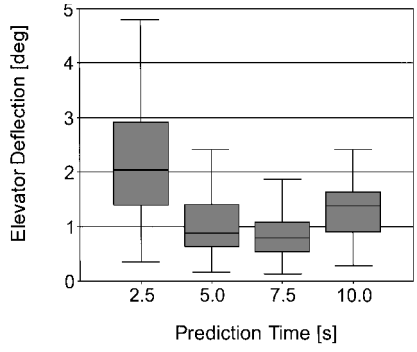

Fig. 12 Pilot control activity (extended predictor concept).

The prediction time T_{PR}, which has been found to be a primary factor for predictor design, has a significant effect on control performance. Results of the simulation experiments for compensatory control of the predictor position are presented in Fig. 11 (box plot technique, 95% confidence interval). This figure shows as a basic result that the predictor position is effectively controlled by the pilot. The deviations of the predictor position from the command flight path are rather small. Pilots ratings are very favorable and supporting the perspective flight-path predictor as an efficient means for improving aircraft guidance and control. Further, Fig. 11 shows that the effect of the prediction time T_{PR} manifests in an increase of the deviations when T_{PR} is increased.

Results on control activity of the pilot are presented in Fig. 12. There is again a strong effect of the prediction time T_{PR}, which now leads to a decrease of the control activity with an increase of T_{PR} and vice versa.

The results presented in Figs. 11 and 12 concerning the effects of T_{PR} can be explained with pilot loop-closure behavior. The reason underlying these effects is graphically illustrated in Fig. 13, which schematically shows frequency responses for two predictor numerator zeros $1/T_{1,a}$ and $1/T_{1,b}$. The change in the numerator zeros is caused by a change of the prediction time from $T_{PR,a}$ to $T_{PR,b}$ because $T_{1,a} \approx T_{PR,a}$ and $T_{1,b} \approx T_{PR,b}$. Figure 13 shows that a numerator zero increase from $1/T_{1,a}$ to $1/T_{1,b}$ yields a change of the K/s frequency region, which is shifted downward (dashed line). The decrease of the effective gain in the K/s frequency region from K_a to K_b is given by (Fig. 13)

$$K_b/K_a \approx T_{1,b}/T_{1,a} \approx T_{PR,b}/T_{PR,a} \tag{24}$$

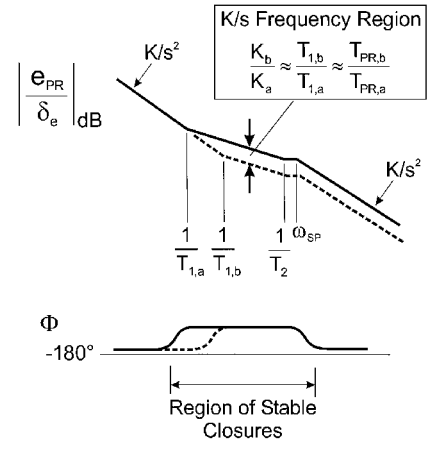

Fig. 13 Effect of prediction time on frequency responses (extended predictor concept): - - - -, T_{PR} decreased (from $T_{PR,a}$ to $T_{PR,b}$).

For loop closure the downward shift of the K/s frequency region requires an increase of pilot gain (from $K_{P,a}$ to $K_{P,b}$), which is approximately the inverse of the ratio expressed in Eq. (22):

$$K_{P,b}/K_{P,a} \approx T_{PR,a}/T_{PR,b} \tag{25}$$

A quantitative evaluation using data from the simulation experiments supports the explanation of the described pilot-closure behavior. Figure 14 shows two frequency responses of the predictor-aircraft system, one for $T_{PR} = 2.5$ s and the other for $T_{PR} = 5.0$ s. Pilot gains, which were estimated from simulation tests, are indicated in Fig. 14. The numerical values of the pilot gains for the two T_{PR} cases correspond with the preceding explanation.

Furthermore, Fig. 14 confirms that the desired K/s goal is achieved. There is a broad K/s frequency region centered around pilot system crossover. Pilot system crossover is near the frequency for maximum phase margin.

The effectiveness of the extended predictor concept for avoiding detrimental turbulence effects was also the subject of experimental verification. Results are presented in Figs. 15 and 16 (Dryden model with rms intensity of 4.7 ft/s for vertical and 4.85 ft/s for longitudinal gusts, according to Refs. 19 and 20). Figure 15 shows that turbulence leads to some increase of the predictor error, which still can be kept at a low level. Correspondingly, the pilot control activity is increased when compared with the case without turbulence (Fig. 16).

Control of Current Position with Predictor

The predictor basically concerns the control of the *future* position at the prediction time ahead (predictor position), $h_{PR} = h(t + T_{PR})$. It will be shown in the following that the predictor is also an efficient means for controlling the *current* position $h = h(t)$, which is the ultimate goal of the control effort of the pilot.

Reference is made to Eq. (15), which relates the future position error indicated by the predictor as $\Delta e_{PR}(s) = K_{PR}\Delta h_{PR}(s)$ to the current flight-path angle rate $\Delta\dot{\gamma}(s)$. Accordingly,

$$\frac{\Delta h_{PR}(s)}{\Delta\dot{\gamma}(s)} = V\frac{(K_q/V)s^2 + T_{PR}s + 1}{s^2} \tag{26}$$

Accounting for $s^2\Delta h(s) = V\Delta\dot{\gamma}(s)$ and selecting T_W and K_q according to Eqs. (14) and (17b), the following relation between the

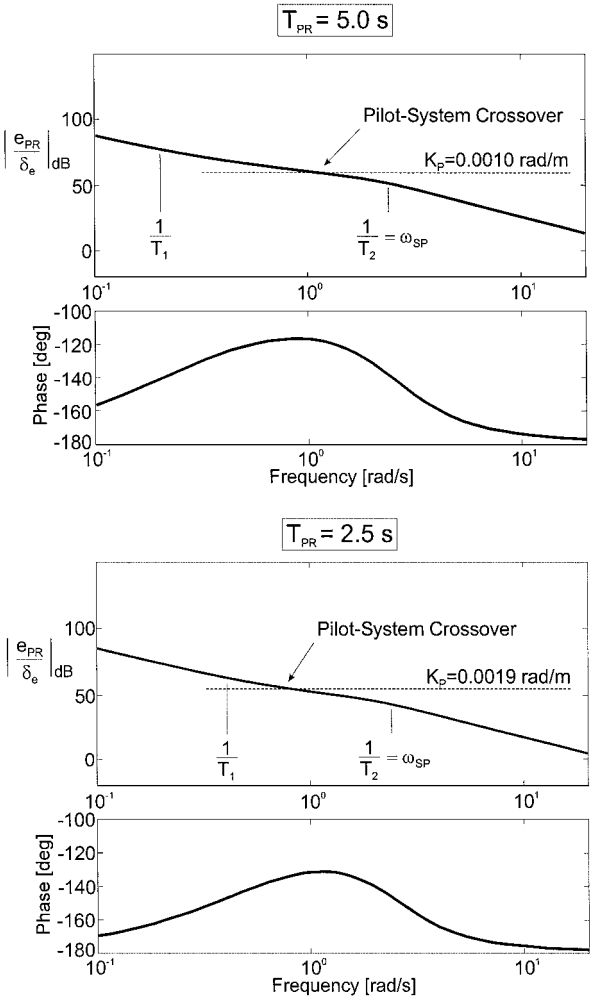

Fig. 14 Frequency responses and pilot gain for crossover.

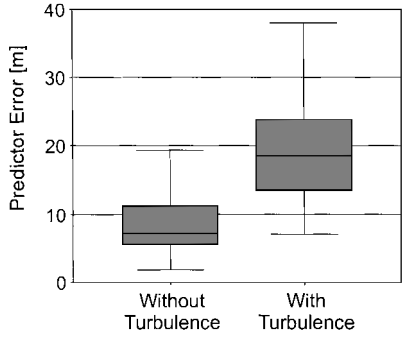

Fig. 15 Effect of turbulence on deviation of predictor position (extended predictor concept, T_{PR} = 5.0 s.)

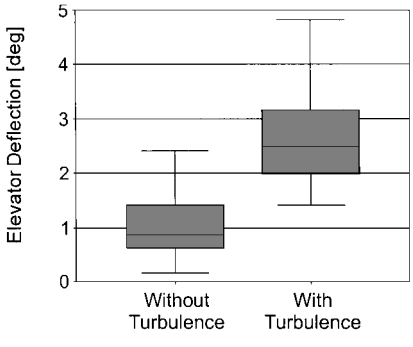

Fig. 16 Effect of turbulence on pilot control activity (extended predictor concept, T_{PR} = 5.0 s.)

current position error $\Delta h(s)$ and the future position error $\Delta h_{PR}(s)$ results:

$$\frac{\Delta h(s)}{\Delta h_{PR}(s)} = \frac{1}{(T_1 s + 1)(T_2 s + 1)} \tag{27}$$

This relation shows that the frequency response has the following property:

$$\left| \frac{\Delta h(s)}{\Delta h_{PR}(s)} \right|_{s = i\omega} \leq 1 \tag{28}$$

As a result, the current position error is basically smaller than the future position error indicated by the predictor. There is a significant reduction of Δh relative to Δh_{PR} in the frequency range just presented $1/T_1$ (20 dB per decade for $\omega \geq 1/T_1$ and 40 dB for $\omega \geq 1/T_2$).

Furthermore, it follows from Eq. (26) that both errors approach the same steady-state value, i.e.,

$$\left. \frac{\Delta h(s)}{\Delta h_{PR}(s)} \right|_{s \to 0} = 1 \tag{29}$$

This means that the current position error becomes zero when the predictor reaches its steady-state reference position, i.e., $\Delta h = \Delta h_{PR} = 0$.

Control of the current position was also the subject of the simulation-test program described in the preceding section. Results are presented in Figs. 17 and 18 (from the same simulation runs as just considered).

A basic result is that the current position can be effectively controlled with the predictor. This holds for both cases graphically illustrated in Figs. 17 and 18. Furthermore, comparison of Fig. 17 with Fig. 11 shows that the current position error is smaller than the predictor position error. Thus, the preceding considerations are confirmed. Another result concerns the prediction time T_{PR}, which has some effect although it appears to be reduced.

The result that the current position error is smaller than the predictor position error also holds for the turbulence case as shown by comparison of Fig. 18 with Fig. 16. Furthermore, Fig. 18 reveals that the error level is similar to the case without turbulence.

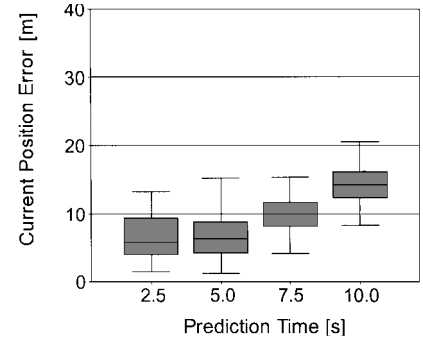

Fig. 17 Deviation of current position (extended predictor concept).

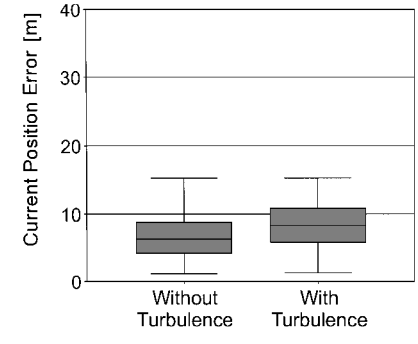

Fig. 18 Effect of turbulence on deviation of current position (extended predictor concept, T_{PR} = 5.0 s.)

Conclusions

A new predictor concept for the longitudinal motion is proposed for enhancing the guidance and control capabilities possible with a perspective flight-path display. The concept is based on manual control issues, appropriately combined with geometric/kinematic relations. Pilot-centered requirements are specified for achieving minimum pilot effort and maximum system performance for manual flight-path control. Key factors of the predictor-aircraft system are identified and optimized for attaining this goal. The new predictor concept requires minimum compensatory effort by the pilot and shows insensitivity to turbulence. It also provides a high degree of face validity, which is considered substantial for a display presenting guidance information in a descriptive and three-dimensional format. Further issues are system stability and response quality. It is shown that not only the future position at a specified time ahead can be effectively controlled but also the current position. The conceptual and theoretical findings are verified with pilot-in-the-loop simulation experiments.

References

[1]Theunissen, E., "Integrated Design of a Man-Machine Interface for 4-D Navigation," Ph.D. Dissertation, Delft Univ. of Technology, The Netherlands, 1997.

[2]Theunissen, E., and Mulder, M., "Availability and Use of Information in Perspective Flightpath Displays," *Proceedings of the AIAA Flight Simulation Technologies Conference*, AIAA, Washington, DC, 1995, pp. 137–147.

[3]Grunwald, A. J., Robertson, J. B., and Hatfield, J. J., "Experimental Evaluation of a Perspective Tunnel Display for Three-Dimensional Helicopter Approaches," *Journal of Guidance, Control, and Dynamics*, Vol. 4, No. 6, 1981, pp. 623–631.

[4]Grunwald, A. J., "Tunnel Display for Four-Dimensional Fixed-Wing Aircraft Approaches," *Journal of Guidance, Control, and Dynamics*, Vol. 7, No. 3, 1984, pp. 369–377.

[5]Grunwald, A. J., "Predictor Laws for Pictorial Flight Displays," *Journal of Guidance, Control, and Dynamics*, Vol. 8, No. 5, 1985, pp. 545–552.

[6]Grunwald, A. J., "Improved Tunnel Display for Curved Trajectory Following: Control Considerations," *Journal of Guidance, Control, and Dynamics*, Vol. 19, No. 2, 1996, pp. 370–377.

[7]Grunwald, A. J., "Improved Tunnel Display for Curved Trajectory Following: Experimental Evaluation," *Journal of Guidance, Control, and Dynamics*, Vol. 19, No. 2, 1996, pp. 378–384.

[8]Haskell, I. D., and Wickens, C. D., "Two- and Three-Dimensional Displays for Aviation: A Theoretical and Empirical Comparison," *International Journal of Aviation Psychology*, Vol. 3, No. 2, 1993, pp. 87–109.

[9]Wickens, C. D., Fadden, S., Merwin, D., and Ververs, P. M., "Cognitive Factors in Aviation Display Design," *Proceedings of the 17th AIAA/IEEE/SAE Digital Avionics Systems Conference*, 1998.

[10]Funabiki, K., Muraoka, K., Terui, Y., Harigae, M., and Ono, T., "In-Flight Evaluation of Tunnel-in-the Sky Display and Curved Approach Pattern," *AIAA Guidance, Navigation, and Control Conference Proceedings*, AIAA, Reston, VA, 1999, pp. 108–114.

[11]Mulder, M., *Cybernetics of Tunnel-in-the-Sky Displays*, Delft Univ. Press, Delft, The Netherlands, 1999, pp. 4–8.

[12]Sachs, G., and Möller, H., "Synthetic Vision Flight Tests for Precision Approach and Landing," *AIAA Guidance, Navigation, and Control Conference Proceedings*, AIAA, Washington, DC, 1995, pp. 1459–1466.

[13]Sachs, G., Dobler, K., and Hermle, P., "Flight Testing Synthetic Vision for Precise Guidance Close to the Ground," *AIAA Guidance, Navigation, and Control Conference Proceedings*, AIAA, Reston, VA, 1997, pp. 1210–1219.

[14]Sachs, G., Dobler, K., and Theunissen, E., "Pilot-Vehicle Control Issues for Predictive Flightpath Displays," *AIAA Guidance, Navigation, and Control Conference Proceedings*, AIAA, Reston, VA, 1999, pp. 574–582.

[15]Sachs, G., Dobler, K., and Theunissen, E., "Pilotengerechte Prädiktorauslegung für Perspektivische Flugbahn-Displays," *DGLR-Jahrbuch 1999, Deutsche Gesellschafft für Luft- und Raumfahrt*, Vol. 2, 1999, pp. 695–704.

[16]Hess, R. A., and Gorder, P. J., "Design and Evaluation of a Cockpit Display for Hovering Flight," *Journal of Guidance, Control, and Dynamics*, Vol. 13, No. 3, 1990, pp. 450–457.

[17]McRuer, D. T., "Pilot Modeling," AGARD-LS-157, 1988, pp. 2-1–2-30.

[18]Hess, R. A., "Feedback Control Models—Manual Control and Tracking," *Handbook of Human Factors and Ergonomics*, 2nd ed., Wiley, New York, 1997, pp. 1249–1294.

[19]MIL-F-8785C, "Flying Qualities of Piloted Airplanes," Sept. 1991.

[20]MIL-HDBK-1797, "Flying Qualities of Piloted Aircraft," Dec. 1997.